Random Generation of Coherent Solitary Waves from Incoherent Waves

Mingzhong Wu,[1] Pavol Krivosik,[1,2] Boris A. Kalinikos,[1,3] and Carl E. Patton[1]
[1]*Department of Physics, Colorado State University, Fort Collins, Colorado 80523, USA*
[2]*Slovak University of Technology, Bratislava, Slovakia*
[3]*St. Petersburg Electrotechnical University, 197376, St. Petersburg, Russia*
(Received 14 March 2006; published 9 June 2006)

The random generation of coherent solitary waves from incoherent waves in a medium with an instantaneous nonlinearity has been observed. One excites a propagating incoherent spin wave packet in a magnetic film strip and observes the random appearance of solitary wave pulses. These pulses are as coherent as traditional solitary waves, but with random timing and a random peak amplitude.

DOI: 10.1103/PhysRevLett.96.227202 PACS numbers: 75.30.Ds, 05.45.−a, 76.50.+g, 85.70.Ge

A solitary wave is a localized large-amplitude pulse excitation in a nonlinear dispersive system that can travel with constant shape and velocity. Such waves can occur in a large number of different physical systems [1–4]. The formation of these solitary waves, however, involve a common process, namely, the compensation of the dispersion (or diffraction) induced pulse broadening by the nonlinearity induced pulse narrowing. For many years solitary waves generally have been taken as *coherent* entities. In recent years, however, there has been increased interest in the formation of *incoherent* solitary waves from *incoherent* waves [5–12]. The concept of incoherent solitary waves was suggested as early as in 1977 [5]. The experimental observation of such incoherent solitary waves, however, has taken nearly 20 years to be realized [6].

This realization was first achieved for the special case of optical spatial solitons. It is important to note that solitons represent a special class of solitary waves that have the further ability to survive collisions with other solitons. Specifically, it was found that incoherent spatial solitons could be formed from spatially and temporally incoherent light beams [6–8]. For the formation of such incoherent spatial solitons, the medium must have a *noninstantaneous* nonlinearity, or a nonlinear response time that is much longer than the time scale for the change of the speckle pattern across the beam. Here, the nonlinearity responds to the time averaged spatial envelope of the beam cross section, not to the localized instantaneous speckle regions in the beam. Very recently, incoherent solitons have also been observed in media with an *instantaneous* nonlinearity, or a nonlinear response time that is much shorter than the correlation time of the incoherent waves [11]. Here, domain-wall type incoherent solitons were formed from two copropagating incoherent light waves in an optical fiber system.

This Letter reports on the formation of temporal solitary waves from *incoherent* waves in a medium with an *instantaneous* nonlinearity. It is found that if one excites a temporal packet of incoherent waves in a one-dimensional nonlinear dispersive medium, a fundamentally new type of solitary wave, a *random solitary wave* (RSW), can be formed from the propagating wave packet. Here, ''random'' means three things. The RSW pulses materialize from the propagating wave packet (1) randomly in time, (2) randomly in position relative to the overall wave packet, and (3) with a random amplitude. In spite of the incoherent nature of the propagating wave packet and the random nature of the generation process, the RSW pulses show coherent properties of the sort found for traditional solitary waves. These results demonstrate the first realization of *coherent* solitary waves from *incoherent* waves.

The experiment utilized spin wave excitations in a long and narrow magnetic film strip of low-loss yttrium iron garnet (YIG). The geometry was set to allow the propagation of spin waves with attractive nonlinearity and support the formation of bright spin wave solitons [13–15]. One first uses a pulse of broadband microwave noise to excite an incoherent spin wave packet at one end of the film strip. One then can trace the propagation of the packet along the strip. The correlation time of the incoherent spin wave packet is determined by the bandwidth of the spin wave signal. The nonlinear response time of the film is inversely proportional to the power of the spin wave signal [13,16]. When the spin wave amplitude is sufficiently large to push the nonlinear response time below the correlation time, one can realize an instantaneous nonlinear response and observe spin wave RSW pulses.

Figure 1 shows the experimental setup and selected signal characteristics. The YIG strip in Fig. 1(a) is magnetized to saturation by a static magnetic field parallel to the length of the strip. This configuration supports the propagation of backward volume spin waves [17] that have an attractive nonlinearity. Three microstrip transducers are placed over the YIG strip. One is used for excitation and the other two are used for detection, as indicated. The noise source, fast switch, and broadband microwave amplifier provide well-defined noise pulses. The input noise pulses excite incoherent propagating spin wave packets in the film. The detected propagating spin wave signals are analyzed with a broadband real time microwave oscilloscope.

 © 2006 The American Physical Society

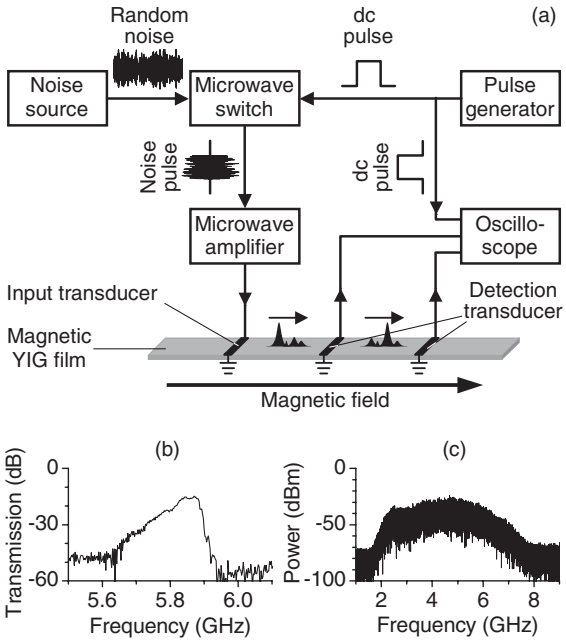

FIG. 1. (a) Schematic of the experimental arrangement based on a magnetic yttrium iron garnet (YIG) film strip. (b) Transmission vs frequency response for the YIG film/transducer structure. (c) Power frequency spectrum for the noise signal.

For the signal characteristics in Fig. 1(b) and 1(c) and the data below, the YIG film strip was 6.8 mm thick, 2.2 mm wide, and 46 mm long. The static magnetic field was 1368 Oe. The microstrip transducers were 50 mm wide and 2 mm long. The detection transducers were held at displacements (x) of 5.3 mm and 10.6 mm from the input transducer. The input noise pulses had a maximum power level of 5 W, durations of several tens of nanoseconds, and a repetition rate of 6 kHz.

Figure 1(b) shows the low-power transmission versus frequency response for the structure. The profile shows a spin wave passband from about 5.7 GHz to about 5.9 GHz. Figure 1(c) shows the power frequency spectrum for the original noise signal. The spectrum shows a noise band from about 2 GHz to about 7 GHz, much wider than the spin wave passband. The noise input bandwidth is adequate, therefore, to excite spin waves over the full spectrum of available modes.

Figure 2 shows the random nature of the observed RSW pulses. Figure 3 shows the characteristics of the RSW pulses. Graph pairs (a)–(c) in Fig. 2 show three sets of output power profiles sampled for three different input noise pulses, each with a duration of 50 ns and a power level of about 5 W. In each graph pair, the left and right graphs show single shot oscillograms at the $x = 5.3$ mm and $x = 10.6$ mm detection positions, as indicated. The shadings show the time windows over which there is bona fide spin wave signal power at the detection point. On an expanded vertical scale, these regions are distinct. The labels A, B, and C serve to identify the RSW pulses.

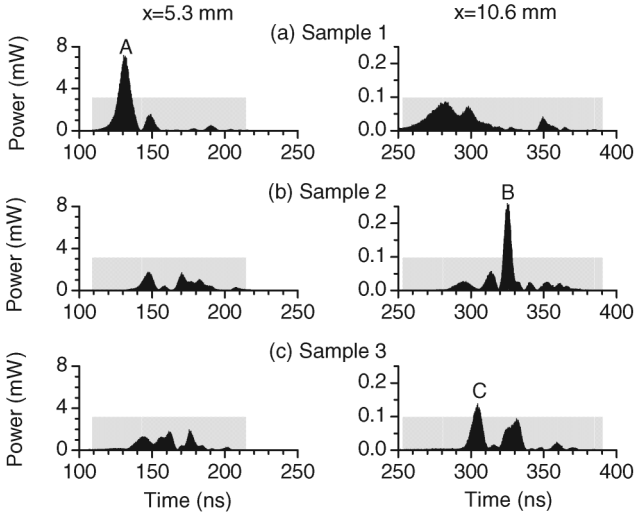

FIG. 2. Graph pairs (a)–(c) show three sets of output power profiles sampled for three different input noise pulses, each with a duration of 50 ns and a power level of about 5 W. The left and right graphs show single shot signals at the two different detection positions, as indicated. The shadings show the time windows for detectable spin wave signal power. The A, B, and C labels identify the pulses that are solitary waves.

Figure 2 shows three key results. First, one can see that the overall wave packets at the two detection positions are much wider than the initial input pulse. As shown by the shadings, the overall signal time windows for the full signal response at $x = 5.3$ mm and $x = 10.6$ mm are about 105 ns and 138 ns, respectively. This indicates that the input incoherent spin wave packet disperses significantly during its propagation along the film strip. Second, one can see that for a given input noise pulse, *the solitary waves*

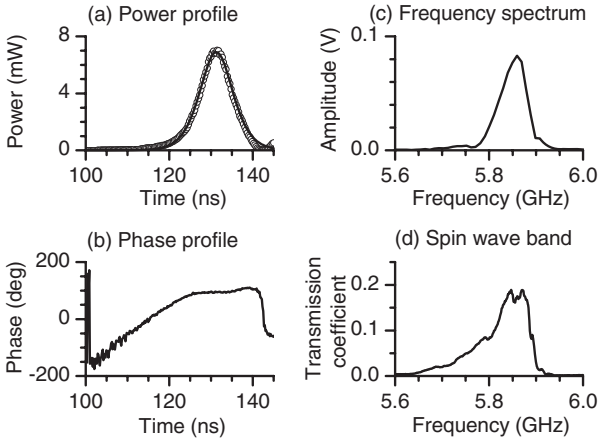

FIG. 3. Expanded time view of pulse A in Fig. 2(a) along with phase and frequency characteristics. (a) Measured power profile (empty circles) and a fit to a hyperbolic secant squared function (curve). (b) Relative phase vs time profile. (c) Frequency spectrum. (d) Transmission coefficient vs frequency response of the YIG film/transducer structure.

that are realized appear randomly. In sample 1, for example, one sees a leading solitary wave pulse (labeled A) at $x = 5.3$ mm but no solitary waves at $x = 10.6$ mm. For sample 2, in contrast, there are no solitary wave pulses at $x = 5.3$ mm, while at $x = 10.6$ mm, one finds a solitary wave (labeled B) in the middle of the signal time window. In sample 3, there are several weak pulses but no solitary waves at $x = 5.3$ mm, while the trace for $x = 10.6$ mm shows a leading solitary wave (labeled C) and a follow-on nonsolitary pulse. Third, the overall signal time window power profile and the appearance of solitary waves *are completely random* from sample to sample. If the measurements are extended to more input noise pulses, each gives a totally different response.

Figure 3 shows details on the characteristics of pulse A in Fig. 2(a). Graph (a) shows the measured power profile (empty circles) on an expanded time scale and a hyperbolic secant squared functional fit to these data (curve). Graphs (b) and (c) show the relative phase profile and frequency spectrum for the pulse, respectively. The phase change in (b) is measured relative to a reference cw signal [15]. The frequency spectrum is obtained through a fast Fourier transform analysis of the signal pulse. Graph (d) shows the transmission coefficient versus frequency response of the structure. This is the same as in Fig. 1(b), but with a linear vertical scale. This response serves as a basis of comparison between the frequency spectrum of the RSW pulse and the spin wave passband.

Figure 3 shows that pulse A actually constitutes a solitary wave. Graph (a) shows that the envelope of the pulse can be nicely fitted to the hyperbolic secant form expected for solitary waves [1,2]. Graph (b) shows that the phase of the pulse is constant across the central portion of the pulse, another key solitary wave property [15,18]. Graphs (c) and (d) show that the frequency spectrum of the pulse matches closely to the spin wave passband for the YIG strip. This match indicates that the RSW pulse formation involves modes over the entire spin wave passband. This is in contrast with traditional solitary waves that are formed with narrow band input pulses. Moreover, both the phase profile and the frequency spectrum appear smooth, clean, and noise free. These data show that one can use a wide band noise input and produce solitary waves that are as coherent and well behaved as traditional solitary waves. This is a fourth key result.

The data in Figs. 2 and 3 demonstrate the generation of coherent solitary waves from incoherent waves and the random nature of the generation process. The physical process for such RSW generation may be described as follows. First, the propagating incoherent spin wave packet consists of a range of uncorrelated spin wave modes. Second, at different times along the propagation path, these uncorrelated modes experience different degrees of constructive interactions that lead to the formation of strong or weak localized spin wave pulses. Third, for the strong pulses, one has a nonlinear response time T_n of the YIG film that is shorter than the correlation time T_c of the spin wave modes and the pulse can evolve into a solitary wave quickly. Once realized, the solitary wave is coherent over a time interval that is shorter than the correlation time.

The nonlinear response time T_n and the correlation time T_c can be estimated through the relations $N|u|^2T_n = \phi_d$ and $T_c = 1/\Delta f$, respectively, where N is a nonlinearity coefficient, $|u|^2$ represents the spin wave power, ϕ_d is the dispersion-induced phase shift across the pulse width, and Δf is the half-power width of the spin wave passband. Information on the nonlinear response of spin waves and the definitions of the corresponding parameters are given in Refs. [13,15]. For the situation in Figs. 2 and 3, the nonlinear response time and the correlation time are estimated to be $T_n \approx 1$–5 ns and $T_c \approx 17$ ns, respectively. These times are consistent with the scenario given above.

One simple test of the $T_n < T_c$ RSW formation hypothesis is to reduce the input power. For weak spin wave pulses, T_n is relatively long and the pulses cannot acquire enough nonlinear phase shift to develop into solitary waves within the correlation time. Figure 4 shows single shot output signals for an input noise pulse at a low-power level of about 0.2 mW. The other conditions were the same as for the data in Figs. 2 and 3. The upper and lower graphs show power and phase profiles, respectively. The power versus time profiles in Fig. 4 are somewhat similar to those in Fig. 2. These data demonstrate the random nature of the spin wave pulse formation process, even for low-power signals.

However, the phase data in Fig. 4(b) are in stark contrast with the corresponding high power data in Fig. 3(b). For a low-power noise pulse input, the phase profiles of the random spin wave pulses are all concave downward, just as one would expect for linear pulses with positive dispersion [15]. These low-power data indicate that a short nonlinear response time and an instantaneous nonlinearity are

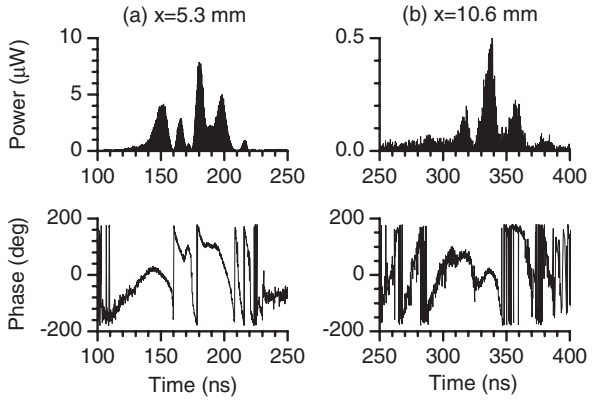

FIG. 4. Output power and relative phase profiles for a 50 ns wide input noise pulse with a power level of about 0.2 mW. The left and right graphs are for two different detection positions, as indicated.

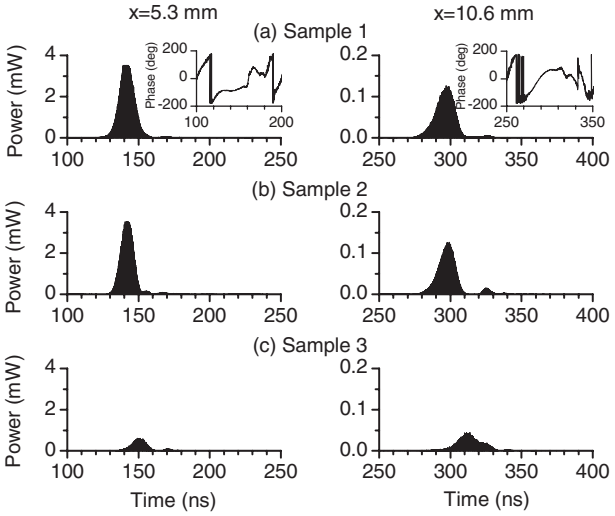

FIG. 5. Graph pairs (a)–(c) show three sets of output power profiles sampled for three separate input noise pulses. The input pulses had a duration of 10 ns and a power level of about 5 W. The left and right graphs show single shot signals at the two different detection positions, as indicated. The insets in (a) show the phase data for the corresponding power profiles.

required for the formation of coherent RSW pulses from incoherent waves.

Turn now to the random nature of the RSW generation process. One explanation for this randomness lies in the fact that the correlation time T_c of the spin wave modes is much shorter than the temporal width T_p of the overall spin wave packet. For the situation in Figs. 2 and 3, the time window T_p is in the 100–140 ns range. When the condition $T_c < T_p$ is satisfied, the spin wave modes randomly change their phase and, hence, interact with each other randomly on any time scale greater than the correlation time. This leads to the random nature of the observed RSW generation, both spatially and temporally.

The above scenario may be tested through the use of short input noise pulses. In this case, the condition $T_c > T_p$ will apply, and one should produce quasicoherent spin wave packets. One will then have stable interactions between the spin wave modes. The realized solitary waves will then have more-or-less traditional solitary wave characteristics. This expectation was tested through a repeat of the Figs. 2 and 3 experiments, but with 10 ns wide input noise pulses.

Figure 5 shows the results. The format is the same as for Fig. 2. The insets in Fig. 5(a) show the phase data for the corresponding power profiles. From top to bottom, one sees that single shot data for three input pulses give different signals. The pulses in Fig. 5(a) and 5(b)are solitary waves. The pulses in Fig. 5(c) are not. As in Fig. 2, one sometimes obtains a solitary wave and sometimes not. The constant phase profiles shown in the insets clearly demonstrate the solitary wave nature of the corresponding pulses. From left to right, however, one sees that for a given input pulse the signals at different positions are more-or-less the same. This means that, when realized, the solitary waves can be tracked from one observation point to another. These data support the thesis that short correlation times relative to the packet width are needed in order to obtain RSW pulses.

This work was supported in part by the U. S. Army Research Office, MURI Grant No. W911NF-04-1-0247, and the Russian Foundation for Basic Research, Grant No. 05-02-17714. Professor Y. S. Kivshar of the Australian National University and Dr. O. Cohen of the University of Colorado are acknowledged for helpful comments.

[1] M. J. Ablowitz and H. Segur, *Solitons and the Inverse Scattering Transform* (SIAM, Philadelphia, 1985).
[2] Y. S. Kivshar and G. P. Agrawal, *Optical Solitons* (Academic, New York, 2003).
[3] K. E. Strecker, G. B. Partridge, A. G. Truscott, and R. G. Hulet, Nature (London) **417**, 150 (2002).
[4] S. O. Demokritov, A. A. Serga, V. E. Demidov, B. Hillebrands, M. P. Kostylev, and B. A. Kalinikos, Nature (London) **426**, 159 (2003).
[5] A. Hasegawa, Phys. Fluids **20**, 2155 (1977).
[6] M. Mitchell, Z. G. Chen, M. F. Shih, and M. Segev, Phys. Rev. Lett. **77**, 490 (1996).
[7] M. Mitchell and M. Segev, Nature (London) **387**, 880 (1997).
[8] Z. G. Chen, M. Mitchell, M. Segev, T. H. Coskun, and D. N. Christodoulides, Science **280**, 889 (1998).
[9] C. B. Clausen, Y. Kivshar, O. Bang, and P. L. Christiansen, Phys. Rev. Lett. **83**, 4740 (1999).
[10] S. A. Ponomarenko, N. M. Litchinitser, and G. P. Agrawal, Phys. Rev. E **70**, 015603 (2004).
[11] A. Picozzi, M. Haelterman, S. Pitois, and G. Millot, Phys. Rev. Lett. **92**, 143906 (2004).
[12] O. Cohen, G. Bartal, H. Buljan, T. Carmon, J. W. Fleischer, M. Segev, and D. N. Christodoulides, Nature (London) **433**, 500 (2005).
[13] M. Chen, M. A. Tsankov, J. M. Nash, and C. E. Patton, Phys. Rev. B **49**, 12 773 (1994).
[14] A. N. Slavin, B. A. Kalinikos, and N. G. Kovshikov, in *Nonlinear Phenomena and Chaos in Magnetic Materials*, edited by P. E. Wigen (World Scientific, Singapore, 1994), Chap. 9.
[15] J. M. Nash, P. Kabos, R. Staudinger, and C. E. Patton, J. Appl. Phys. **83**, 2689 (1998).
[16] M. A. Tsankov, M. Chen, and C. E. Patton, J. Appl. Phys. **76**, 4274 (1994).
[17] P. Kabos and V. S. Stalmachov, *Magnetostatic Waves and Their Applications* (Chapman & Hall, London, 1994).
[18] B. A. Kalinikos, N. G. Kovshikov, and C. E. Patton, Phys. Rev. Lett. **78**, 2827 (1997).